Seitz, F.; Kutterer, H.: Sensitivity analysis of the non-linear Liouville equation.

In: Sansò, F. (Ed.) A Window on the Future of Geodesy, IAG Symposia, Vol. 128, 601-606, Springer, ISBN (Print) 978-3-540-24055-6, ISBN (Online) 978-3-540-27432-2, ISSN 0939-9585, 2005.

DOI: 10.1007/3-540-27432-4_102, 2005

In: A Window on the Future of Geodesy, F. Sansó (Ed.),
IAG Symposia, Vol. 128, Springer, Berlin, 601-606, 2005.

Sensitivity Analysis of the Non-Linear Liouville Equation

Florian Seitz, Hansjörg Kutterer
Deutsches Geodätisches Forschungsinstitut (DGFI), Marstallplatz 8, D-80539 Munich, Germany
E-Mail: florian.seitz@dgfi.badw.de

Abstract. The non-linear gyroscopic model DyMEG has been developed at DGFI in order to study the interactions between geophysically and gravitationally induced polar motion and the Earth's free oscillations, particularly with regard to the Chandler wobble. The model is based on a triaxial ellipsoid of inertia and dispenses with any explicit information concerning amplitude, phase, and period of the Chandler oscillation. The characteristics of the Earth's free polar motion is reproduced by the model from rheological and geometrical parameters. Therefore, the traditional analytical solution is not applicable and the Liouville equation is solved numerically as an initial value problem. The gyro is forced by consistent atmospheric and oceanic angular momentum. Mass redistributions are able to take influence on the free rotation via rotational deformations. In order to assess the dependence of the numerical results on the initial values and rheological or geometrical input parameters like the Love numbers and the Earth's principal moments of inertia, a sensitivity analysis has been performed. The study reveals that the most critical parameter in the model is the pole tide Love number k_2 whereas the dependence of the solution on the other mentioned parameters is marginal.

Keywords. Earth Rotation, Gyroscopic Model, Liouville Differential Equation, Critical Parameters, Sensitivity Analysis.

1 Introduction

The non-linear gyroscopic model DyMEG (Dynamic Model for Earth Rotation and Gravity) has been developed at DGFI in order to study the dynamics of the Earth system based on the interactions between its individual components. Among the latter are the atmosphere, the oceans, and the solid Earth as well as extraterrestrial bodies like sun and moon.

Mass redistributions outside and inside the Earth which are due to geophysical processes and gravitational influences of celestial bodies affect the Earth's rotation on sub-daily to secular time scales and manifest in polar motion and length-of-day variations (ΔLOD). The effects of these excitations are superposed by free oscillations of the Earth such as, e.g. the Chandler wobble.

DyMEG is based on the balance of angular momentum in the Earth system. The characteristics of Earth rotation is generated based on rheological and geometrical parameters. As no explicit information about amplitude, phase, and period of the Earth's free polar motion is provided, the Liouville differential equation has to be solved numerically, e.g. by means of a Runge-Kutta-Fehlberg method (Seitz and Kutterer, 2002; Seitz et al., 2003). In the present investigation, the sensitivity of the solution is discussed with respect to numerical parameters which are entered into the model. In particular, the effects of the pole tide Love number k_2, the initial values for the numerical solution and the modification of the initial tensor of inertia of the basic Earth model are discussed.

2 Configuration of DyMEG

2.1 Liouville Differential equation

In a geocentric reference frame which rotates uniformly and performs one revolution per sidereal day about its *z*-axis, the Earth's reaction on mass redistributions can be described by the Liouville differential equation:

$$\frac{\mathrm{d}}{\mathrm{dt}}\left(\underline{\mathbf{I}}\,\boldsymbol{\omega} + \mathbf{h} \right) + \boldsymbol{\omega} \times \left(\underline{\mathbf{I}}\,\boldsymbol{\omega} + \mathbf{h} \right) = \mathbf{L}\,. \qquad (1)$$

The rotation axis *z* of the reference frame which is also known as *nutation frame* (Moritz and Mueller, 1987) is oriented approximately towards the direction of the maximum moment of inertia *C*. In Eq. (1), the

Earth rotation vector is given by $\boldsymbol{\omega}(t) = \Omega \cdot (m_1(t), m_2(t), 1 + m_3(t))$, where the small dimensionless quantities m_i (i = 1,2,3) denote deviations from the uniform rotation of the nutation frame with the angular velocity Ω.

Geophysical and gravitational forces yield changes of the instantaneous distribution of masses in individual system components. They are reflected in changes of the Earth's tensor of inertia $\underline{\mathbf{I}}(t)$ and relative angular momentum $\mathbf{h}(t)$ which is due to the motion of mass elements with respect to the rotating reference frame. The vector $\mathbf{L}(t)$ on the right hand side of Eq. (1) denotes torques which are due to direct gravitational forces of Sun and Moon.

The tensor of inertia $\underline{\mathbf{I}}(t)$ is composed of two additive components $\underline{\mathbf{I}}_0$ and $\Delta\underline{\mathbf{I}}(t)$, where $\underline{\mathbf{I}}_0$ is the invariant tensor of inertia of the basic Earth model. With respect to the principal axes of inertia of the model body, $\underline{\mathbf{I}}_0$ is given by

$$\underline{\mathbf{I}}_0 = \begin{pmatrix} A & 0 & 0 \\ 0 & B & 0 \\ 0 & 0 & C \end{pmatrix}, \qquad (2)$$

where A and B are the equatorial principal moments of inertia ($C>B>A$). $\Delta\underline{\mathbf{I}}(t)$ contains perturbations of $\underline{\mathbf{I}}_0$ due to mass redistributions. The principal axes of inertia and the axes of the nutation frame do not coincide as the axis of the maximum equatorial moment of inertia A points approximately towards 345° longitude (Marchenko and Schwintzer, 2003). This divergence is taken into account by means of a rotation. The dependence of the numerical solution on the choice of the values for A, B, and C as well as of the orientation of the principal axes of inertia is assessed in this paper.

2.2 Free rotation of the gyroscopic model

Within the present study, the interactions between forced and free oscillations of the Earth shall be investigated. Therefore, the traditional analytical approach is not applicable as the Earth's free polar motion is produced by the gyroscopic model from rheological and geometrical parameters (Seitz et al, 2003).

The free rotation of the Earth is lengthened from the Euler period of 304 days (which would be the period if the Earth was rigid) to the observed Chandler period of about 434 days due to the influence of rotational deformations (pole tides). This back-coupling mechanism of rotational variations causes perturbations in the second degree spherical harmonic geopotential coefficients ΔC_{21} and ΔS_{21} (McCarthy, 2003) which are directly linked to $\Delta\underline{\mathbf{I}}(t)$:

$$\Delta C_{21} = -\frac{\Omega^2 a^3}{3GM}\left(\Re(k_2)\cdot m_1 + \Im(k_2)\cdot m_2\right)$$

$$\Delta S_{21} = -\frac{\Omega^2 a^3}{3GM}\left(\Re(k_2)\cdot m_2 - \Im(k_2)\cdot m_1\right)$$

Here, a denotes the Earth's mean equatorial radius, M is the total mass of the Earth and G is the gravitational constant. The effects on the centrifugal potential due to the rheological characteristics of the model body are described by the complex pole tide Love number k_2 which comprehends the effects of mantle anelasticity and ocean pole tides. Both period and damping of the Chandler oscillation strongly depend on the value of k_2. Its influence on the numerical result is discussed within this study.

In the following, a simple Earth model is employed. It consists of an anelastic mantle and a spherical liquid core which are assumed to be fully decoupled. For investigations on polar motion, this simplification is justified on time scales which are longer than one day (Brzezinski, 2001). Therefore, the principal moments of inertia A, B, and C in Eq. (2) are replaced by A_m, B_m, and C_m which are attributed to the mantle alone (Sasao et al., 1980).

Initial values m_i ($t=t_0$) for the first time step are deduced from the geodetically observed time series C04 of the IERS. The transformation between the C04-values which record the coordinates of the celestial ephemeries pole (CEP) w.r.t. to the IERS reference pole and m_i was described by Gross (1992).

2.3 Atmospheric and Oceanic excitation

DyMEG is forced by atmospheric and oceanic angular momentum variations. The indirect effect due to load deformations is computed via Green's functions.

For atmospheric and oceanic forcing, two independent consistent model combinations are considered in this study.

First, atmospheric data based on the reanalyses of the National Centers of Environmental Prediction (NCEP) (Kalnay et al., 1996) were applied in combination with the ocean model ECCO (Stammer et al., 2003). The combination NCEP-ECCO is a consistent representation of dynamics and mass redistributions in the subsystems atmosphere and ocean as NCEP forcing fields are used for the computation of ocean dynamics in ECCO. The

simulations cover a range of 23 years between 1980 and 2002.

Second, the atmospheric ECHAM3-T21 GCM (Roeckner et al., 1992) which is driven by observed sea surface temperature (SST) fields was used in combination with the ocean model OMCT for circulation and tides (Thomas et al., 2001) which is driven by ECHAM3. Both models as well as their linkage are described in detail in Seitz et al. (2003). The simulations cover a range of 22 years between 1973 and 1994.

As NCEP is based on atmospheric observations, the combination NCEP-ECCO is expected to sync better with reality than ECHAM3-OMCT. The latter models are completely free and apart from the initial SST-boundary conditions, dynamics of atmosphere and oceans are solely based on model physics. However, it has been shown that resulting polar motion time series from DyMEG are in good agreement with the observations (Seitz et al., 2003).

3 Sensitivity Analysis

3.1 Effect of the pole tide Love number k_2

In order to assess the influence of the pole tide Love number k_2 on polar motion, several model runs were performed which differ with respect to the value of k_2. As DyMEG accounts for the effects of equilibrium ocean pole tides and mantle anelasticity, the effective pole tide Love number k_2 is composed from three additive contributors:

$$k_2 = k_2^* + \Delta k_2^O + \Delta k_2^A$$

Here, k_2^* denotes a Love number which would be appropriate for a purely elastic Earth neglecting the dynamic response of the oceans as well as the influence of mantle anelasticity. The latter effects are taken into account by adding the surcharges Δk_2^O and Δk_2^A, respectively (Smith and Dahlen, 1980). Dynamic effects of the core are neglected as core and mantle are decoupled. In DyMEG, the approximate values k_2^*=0.3, Δk_2^O=0.044, and Δk_2^A=0.012+ 0.0035i (Mathews et al., 2002; McCarthy, 2003) are introduced. As the anelastic response of the mantle on rotational variations is accompanied by energy dissipation, the supplement Δk_2^A is complex. As a consequence, the Chandler wobble is a damped oscillation which would diminish if it was not continuously excited.

In the following, the dependence of the numerical solution on real and imaginary part of k_2 was studied separately. First, $\Re(k_2)$ was increased from 0.3100 to 0.3800 in 36 equidistant steps while $\Im(k_2)$=0.0035 was kept unchanged. DyMEG was forced by atmospheric and oceanic excitation (NCEP+ECCO) including loading and tidal deformations during 1980 and 2002. In Fig. 1 the resulting time series for polar motion (x-component) are shown against the range of $\Re(k_2)$. As both annual and Chandler wobble are almost circular, the y-component looks alike.

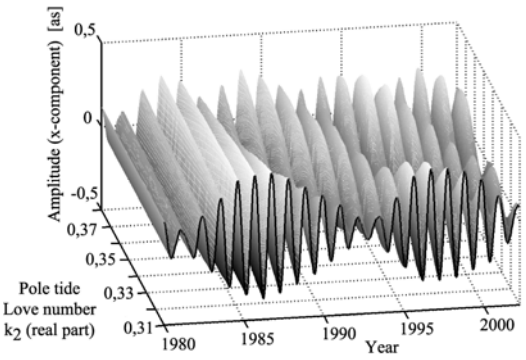

Fig. 1: Resulting time series for polar motion (x-component) for NCEP+ECCO forcing. The model runs differ with respect to the real part of k_2.

As clearly visible, the real part of k_2 takes influence on both the period and the amplitude of the Chandler oscillation and therefore causes a shift of the characteristic beat of free and forced oscillations. From spectral analyses of the time series by means of fourier transformation, the relation between $\Re(k_2)$ and the Chandler period was obtained (Fig. 2, solid black line). Maximum agreement between the observed Chandler period of 434 days and the model is reached for $\Re(k_2)$=0.3520. Here, the correlation between the model time series for polar motion and C04 reaches 0.97. The relation between the Chandler period of the NCEP+ECCO forced model simulations and $\Re(k_2)$ is obviously non-linear.

In order to examine the reason for the non-linear relationship, the experiment was repeated without any forcing, i.e. only the effect of rotational deformations was regarded. Then DyMEG produces a damped oscillation with periods between 400 and 455 days, respectively. The resulting relation between $\Re(k_2)$ and the Chandler period (Fig. 2, dotted black line) is linear. Accordingly, the non-linear behaviour in the NCEP+ECCO case is due to

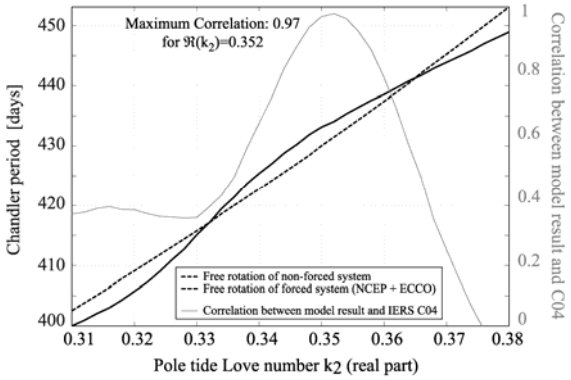

Fig. 2: Relation between $\Re(k_2)$ and the Chandler period as produced by DyMEG in case of forced and unforced conditions. Maximum correlation (scale on the right) is reached for $\Re(k_2)$=0.3520.

the interaction of free and forced polar motion. A similar relation between $\Re(k_2)$ and the Chandler period was derived from ECHAM+OMCT forced model runs. Neither in NCEP+ECCO nor in ECHAM+OMCT there is increased excitation power in the Chandler frequency band. Nevertheless, there is a significant impact on the Chandler period.

A similar analysis was performed for the imaginary part of k_2. The value of the real part was set to 0.3520. The imaginary part $\Im(k_2)$ was increased equidistantly from 0 (no damping) to 0.0060. A small value for $\Im(k_2)$ causes an only slow decrease of the Chandler amplitude. Vice versa, a large value for $\Im(k_2)$ leads to a strong diminution of the Chandler wobble after few years. Unforced results of DyMEG feature damped oscillations which have a constant period of 434 days but differ with respect to the damping. In general, damping is expressed in terms of a so-called quality factor Q. From the damped oscillations of the unforced results, the Q-factor was assessed by a least squares fit (Seitz et al., 2003). For $\Im(k_2)$=0, the Q-factor goes to infinity, for $\Im(k_2)$=0.0060 its value is 48 (Fig. 3).

In order to assess the optimum damping for the NCEP+ECCO forced system, an annual oscillation with constant amplitude and a Chandler oscillation with a period of 434 days together with a rate were fit to the model result by means of least squares adjustment. The resulting Chandler rates from each model run were compared with the respective value derived from C04 for the time between 1980 and 2002 (Fig. 3). Optimum agreement was achieved for $\Im(k_2)$=0.0042 which corresponds to a quality factor of Q=69. The observed rate of the Chandler wobble between 1980 and 2002 is $-1\text{x}10^{-3}$ as/a.

For ECHAM+OMCT, maximum agreement was reached for $\Im(k_2)$=0.0043 (Q=68) between 1975 and 1994. Hence, the power of the respective excitation series seems slightly higher in this case. Anyhow the difference between both model runs is marginal.

Summing up the above results, the pole tide Love number k_2 which will be used in the further investigations with DyMEG is set to 0.3520+0.0042i.

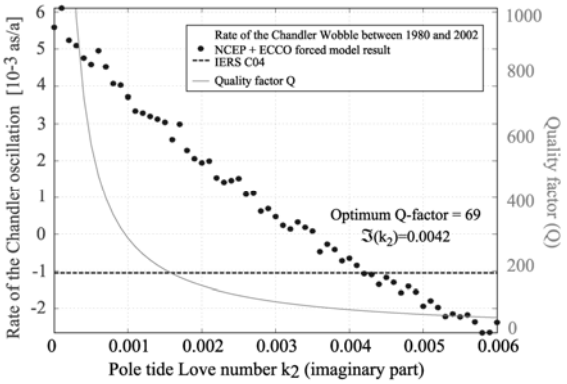

Fig. 3: Relation between the rate of the Chandler amplitude between 1980 and 2002 and $\Im(k_2)$. Optimum agreement between C04 (dotted) and the model result is achieved for $\Im(k_2)$=0.0042 (Q=69).

3.2 Effect of the initial values

In DyMEG, the Liouville differential equation is solved by numerical integration. Hence, initial values $m_i(t=t_0)$ for the first time step have to be provided. As mentioned above, the initial values are deduced from the C04 series of the IERS. In order to assess the effect of inaccurate initial values on the solution, each of the $m_i(t=t_0)$ was independently varied by means of uniformly distributed random numbers between $\pm 3\sigma_i$ around the respective C04 value. Here, σ_i denotes the standard deviation of each m_i which was calculated from an interval of 30 days around the starting date $t=t_0$. Within this analysis, different starting dates were considered. The simulations were started in half-yearly steps between 1973 until 1994 for ECHAM+OMCT and from 1980 until 2001 for NCEP+ECCO.

As a result, this investigation revealed that the modification of the initial values within the $\pm 3\sigma_i$-interval for a single starting point does not have a large effect on the resulting time series. In general, the results of 30 model runs which were performed for each of the atmosphere-ocean combinations

showed similar results. Deviations of the respective time series between each other are largest at the beginning of the simulations (due to the starting situation). But as convergence increases with time, DyMEG seems to reach a steady state.

In contrast, the choice of the starting date seems to be more critical. Fig. 4 displays RMS values of the difference between the model result and the C04 for polar motion (x-component) as well as the corresponding correlations against the respective starting date of the simulation. The model runs end at 31.12.1994 in the case of ECHAM+OMCT and 1.3.2002 in the case of NCEP+ECCO.

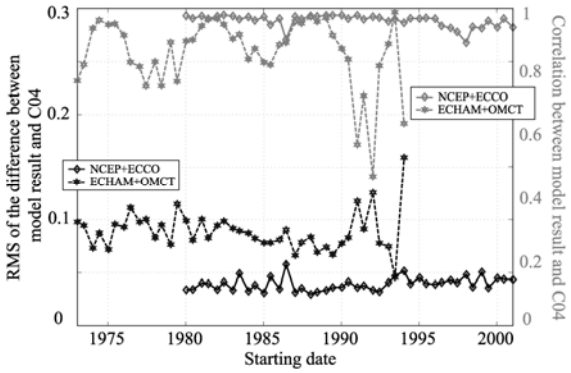

Fig. 4: RMS values of the difference between model results and C04 (black) and respective correlations (grey). The model runs differ with respect to the starting dates.

In general, NCEP+ECCO feature results which are in better agreement with C04 than ECHAM+OMCT. Obviously, there are starting dates which lead to better results than others. For ECCO+NCEP, a start at 1.6.1986 is disadvantageous whereas the neighbouring starting dates lead to good results. For ECHAM+OMCT the correlations feature a clear oscillation which is not visible in the RMS values. This oscillation does not show up in the case of NCEP+ECCO. Accordingly, the amplitudes of polar motion seem to be less affected than phases or frequencies. During the last few years of the respective simulations, the correlations decrease as the considered parts of the polar motion series are rather short. Hence this effect seems to be an artefact.

3.3 Effect of variations in the initial tensor of inertia of the basic Earth ellipsoid

The influence of the choice of $\underline{\mathbf{I}}_0$ on the model results for polar motion was tested in two steps.

First, the model results for a triaxial ellipsoid of inertia ($A \neq B$) were contrasted to a simplified biaxial ($A=B$) solution. NCEP+ECCO forcing was applied in both cases. Although the difference between A and B is marginal, this study revealed that the Chandler period is shortened about two days if a rotationally symmetric basic ellipsoid of inertia is introduced into DyMEG. Vice versa, in order to lengthen the biaxial Chandler period to the value derived from the triaxial approach, the pole tide Love number has to be adopted (cf. 3.1). According to the results of this study, the appropriate value for $\Re(k_2)$ was 0.3550 if a biaxial ellipsoid of inertia is applied. The results are compiled in Table 1.

Table 1. Periods of the free Earth rotation as derived from DyMEG for a biaxial and triaxial basic ellipsoid of inertia in dependence of $\Re(k_2)$

	$\Re(k_2)$ =0.3520	$\Re(k_2)$ =0.3550
$A=B$	432	434
$A \neq B$	434	436

In a second step, the values for A, B, and C were changed as well as the direction of the principal axes of inertia with respect to the axes of the reference frame. Therefore, estimates for the Earth's tensor of inertia were introduced which are based on the recent gravity field solutions JGM-3, EGM96, GRIM5-S1, and GRIM5-S1CH1 (Marchenko and Schwintzer, 2003). In these solutions, the direction $\lambda(A)$ of the principal axis of inertia for the equatorial moment A varies between 345.0709° and 345.0712°. In order to study the sensitivity of DyMEG with respect to $\lambda(A)$, this angle was increased from 344.5° to 345.5° in 50 equidistant steps.

Both experiments, the variation of A, B, and C as well as the variation of $\lambda(A)$ within these reasonable limits did not lead to significant changes of the resulting polar motion series. Therefore these parameters of the basic triaxial tensor of inertia $\underline{\mathbf{I}}_0$ are considered uncritical.

4 Conclusions

The sensitivity of DyMEG with respect to several input parameters as well as the corresponding reliability of the numerical results was assessed within this paper.

The results showed that the model time series strongly depend on the pole tide Love number k_2 with respect to period and damping of the Chandler wobble. From various model runs, the value k_2=0.3520+ 0.0042i was found to yield optimum agreement between the model result for polar motion and the C04 series of the IERS. While the value of the real part of k_2 is in good agreement with recent studies, the value

of the imaginary part slightly differs from the one given in McCarthy (2003).

Note that the sensitivity of the model Chandler period with respect to the real part of k_2 is very high. A change of this value by 1% results in a reaction of the period of about two days. Hence, the conclusion from the Chandler period to $\Re(k_2)$ is relatively precise.

While the variation of the triaxial initial tensor of inertia $\underline{\mathbf{I}}_0$ as well as the modification of the initial values $m_i(t=t_0)$ did not significantly influence the results, the system is sensitive to the starting date. The correlation between successive NCEP+ECCO forced model results and C04 showed only slight variations whereas the ECHAM+OMCT forced results strongly depend on the starting date. The dependency of the quality of the resulting time series on the starting date will be subject to further investigations.

If the simulations are started at advantageous dates, the model results for polar motion are in good agreement with geodetic observations (Fig. 5).

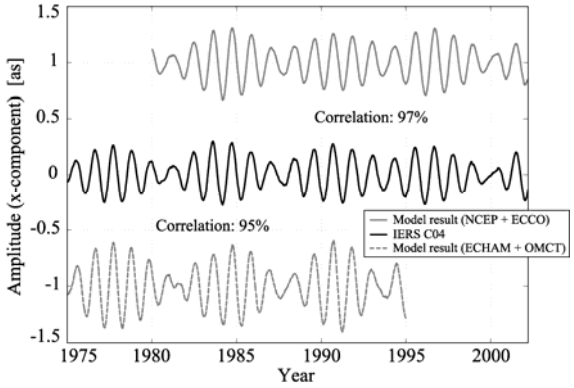

Fig. 5: Model results for DyMEG forced by NCEP+ECCO (top) and ECHAM+OMCT (bottom) in comparison with the geodetic observations C04 (middle). For better comparability, the model results are shifted ±1as.

The correlation between the C04 values and the two displayed model runs is 95% and 97% respectively. As the annual signal of the ECHAM+OMCT result is too strong compared to the observations, the RMS of the difference to C04 is higher than for NCEP+ECCO (cf. Fig. 4). Both polar motion series feature an undamped beat between free and forced polar motion. Hence, the atmospheric and oceanic excitation series are able to maintain the Chandler amplitude.

Acknowledgements

This paper was developed within a project funded by DFG grant DR 143/10. The authors like to thank M. Thomas (Technische Universität Dresden) and J. Stuck (Universität Bonn) for providing OMCT and ECHAM3 data sets. NCEP reanalysis data was provided by the NOAA-CIRES Climate Diagnostics Center, Boulder, Colorado, USA.

References

Brzezinski A. (2001). Diurnal and subdiurnal terms of nutation: a simple theoretical model for a nonrigid Earth. In: Proceedings of the Journées Systémes de Référence Spatio-temporels 2000, pp. 243-251, ed. Capitaine N., Paris.

Gross R. (1992). Correspondence between theory and observations of polar motion. Geophys. J. Int., 109, 162-170.

Kalnay E., Kanamitsu M., Kistler R. et al. (1996). The NCEP/NCAR 40-Year Reanalysis Project. Bull. Amer. Meteor. Soc., 77, 437-471.

Marchenko A., Schwintzer P. (2003). Estimation of the Earth's tensor of inertia from recent global gravity field solutions. J. Geodesy, 76, 495-509.

Mathews P., Herring T., Buffet B. (2002). Modelling of nutation and precession: New nutation series for nonrigid Earth and insights into the Earth's interior. J. Geophys. Res., 107, 10.1029/2001JB000390.

McCarthy D. (2003). IERS Conventions 2000. IERS Technical Note, Paris.

Moritz H., Mueller I. I. (1987). Earth Rotation. Ungar Publishing Company, New York.

Roeckner E., Arpe K., Bengtsson L. et al. (1992). Simulation of the present-day climate with the ECHAM model: Impact of the model physics and resolution. Tech. Rep. No. 93, Max-Planck-Institut für Meteorologie, Hamburg.

Sasao T., Okubo S., Saito M. (1980). A simple theory on the dynamical effects of a stratified fluid core upon nutational motion of the earth. In: Nutation and the Earth's Rotation, eds. Fedorov E., Smith M., Bender, P., IAU Symposia, 78, D. Reidel, Kiev, 165-183.

Seitz F., Kutterer H. (2002). Numerical Solutions for the Non-Linear Liouville Equation. In: Vistas for Geodesy in the New Millennium, eds. Adam J., Schwarz K.-P., IAG Symposia, 125, Springer, Berlin, 463-468.

Seitz F., Stuck J., Thomas M. (2003). Consistent Atmospheric and Oceanic Excitation of the Earth's Free Polar Motion. Submitted to Geophys. J. Int., in review.

Smith M., Dahlen F. (1981). The period and Q of the Chandler wobble. Geophys. J. R. astr. Soc., 64, 223-281.

Stammer D., Wunsch C., Giering R. et al. (2003). Volume, heat and freshwater transports of the global ocean circulation 1993-2000, estimated from a general circulation model constrained by World Ocean Circulation Experiment (WOCE) data. J. Geophys. Res., 108, 10.1029/2001JC001115.

Thomas M., Sündermann J., Maier-Reimer E. (2001). Consideration of ocean tides in an OGCM and its impacts on subseasonal to decadal polar motion excitation. Geophys. Res. Lett., 28, No. 12, 2557-2560.